Available online at www.sciencedirect.com
SCIENCE DIRECT®
European Polymer Journal 41 (2005) 2893–2908
EUROPEAN POLYMER JOURNAL
www.elsevier.com/locate/europolj

Optimal control determination of MMA polymerization in non-isothermal batch reactor using bifunctional initiator

Simant R. Upreti *, Baranitharan S. Sundaram, Ali Lohi

Department of Chemical Engineering, Ryerson University, 350 Victoria Street, Toronto, Ont., Canada M5B 2K3

Received 7 April 2005; received in revised form 14 June 2005; accepted 16 June 2005
Available online 28 July 2005

Abstract

In this work, we determine the optimal control for free-radical methyl methacrylate polymerization using a bifunctional initiator in a non-isothermal batch reactor. A detailed unsteady-state model of the process is employed. Four different optimal control objectives are realized, each of which optimizes a given variable simultaneously with the specification of another. The first two objectives involve the maximization of monomer conversion in a specified operation time, and the minimization of operation time for a specified, final monomer conversion. The last two objectives involve the maximization of monomer conversion for specified, final number and weight average polymer molecular weights. The temperature of heat-exchange fluid inside reactor jacket is considered as a control function of an independent variable. To meet the specification of an optimization variable other than time, the differential model of batch process is derived in the range of specified variable. Equations are provided for Jacobian evaluations to help in the accurate solution of process model. A genetic algorithms-based optimal control method is applied to realize the four optimal control objectives. The results show that optimal control can significantly enhance the performance of the batch polymerization process.

Keywords: Optimal control; Batch reactor; Methyl methacrylate; Polymerization; Bifunctional initiation

1. Introduction

Poly(methylmethacrylate) or PMMA is a transparent thermoplastic, which is extensively used in manufacturing industry because of its high resistance to ultraviolet degradation and corrosion. PMMA is generally produced by the free radical polymerization of methyl methacrylate (MMA) in batch reactors, which are easily adaptable to production demands, and are simple to operate. The performance of batch reactors can be enhanced by optimizing various process parameters that are available for manipulation. Some of these parameters, e.g. the temperature of heat-exchange fluid, can be varied with time in an optimal fashion to achieve what is known as the optimal control of a process. In general, the optimal control of process denotes off-line determination of optimization function(s), the online application of which would achieve a desired objective. It must be noted that optimal control, also referred as dynamic optimization, is neither the usual (closed loop) process control nor optimization, which involves variables but not functions as optimization parameters.

* Corresponding author. Tel.: +1 416 979 5000x6344; fax: +1 416 979 5083.
E-mail address: supreti@ryerson.ca (S.R. Upreti).

0014-3057/$ - see front matter © 2005 Elsevier Ltd. All rights reserved.
doi:10.1016/j.eurpolymj.2005.06.019

Nomenclature

A	heat transfer area, m^2
C_p	specific heat of reactant mixture, J/g K
f	efficiency of initiator
i	concentration of initiator, mol/L
i^0	initial i, mol/L
$\underset{\sim}{i}$	normalized i
$\widetilde{I}$	initiator
J	performance index
K_{d1}	rate coefficient of chemical initiation, min^{-1}
K_{d2}	rate coefficient of chemical initiation with undecomposed radical, min^{-1}
K_p	rate coefficient of propagation, L/mol min
K_t	rate coefficient of termination, L/mol min
$K_{t,c}$	rate coefficient of termination by combination, L/mol min
$K_{t,d}$	rate coefficient of termination by disproportionation, L/mol min
$K_{tf,m}$	rate coefficient of chain transfer to monomer, L/mol min
$K_{tf,s}$	rate coefficient of chain transfer to solvent, L/mol min
$K_{tf,z}$	rate coefficient of chain transfer to inhibitor, L/mol min
m	monomer concentration, mol/L
m^0	initial m, mol/L
$\underset{\sim}{m}$	normalized m
$\underset{\sim}{m}_f$	final $\underset{\sim}{m}$
M	monomer
$\overline{M}_n$	number average molecular weight, g/mol
$\overline{M}_{n,f}$	final, specified $\overline{M}_n$, g/mol
$\overline{M}_w$	weight average molecular weight, g/mol
$\overline{M}_{w,f}$	final, specified $\overline{M}_w$, g/mol
M_m	monomer molecular weight, g/mol
P_l	dead polymer of chain length l
$\widetilde{P}_l$	dead polymer of chain length l, with one undecomposed peroxide
$\widetilde{\widetilde{P}}_l$	dead polymer of chain length l, with two undecomposed peroxide
$R^{\cdot}_{in}$	initiator radical
$\widetilde{R}^{\cdot}_{in}$	initiator radical with one undecomposed peroxide
$R^{\cdot}_l$	radical of chain length l
$\widetilde{R}^{\cdot}_l$	radical of chain length l, with one undecomposed peroxide
$R^{\cdot}_k$	radical of chain length k
$\widetilde{R}^{\cdot}_k$	radical of chain length k, with one undecomposed peroxide
s	solvent concentration, mol/L
s^0	initial s, mol/L
$\underset{\sim}{s}$	normalized s
$\widetilde{S}$	solvent
t	time, min
t_f	final, specified operation time, min
T	temperature of reactants (or reactor), °C
T^0	initial T, °C
T_{max}	upper limit to T, °C
$\underset{\sim}{T}$	normalized T
$\widetilde{T}_j$	temperature of heat exchange fluid in reactor jacket, °C
$T_{j,max}$	upper limit to T_j, °C
$T_{j,min}$	lower limit to T_j, °C
U	heat transfer coefficient for reactor wall and jacket, J/m^2 min K
V	volume of reactants inside reactor, L
V^0	initial V, L
$\underset{\sim}{V}$	normalized V
$\widetilde{X}$	monomer conversion, %
X_f	specified, final X
y_j	jth state variable
z	concentration of inhibitor, mol/L
z^0	initial z, mol/L
$\underset{\sim}{z}$	normalized z
$\widetilde{Z}$	inhibitor
$Z^{\cdot}$	inactive inhibitor radical

Greek symbols

$-\Delta H$	heat of polymerization, J/mol
λ_j	jth moment of live polymer radical
$\underset{\sim}{\lambda}_j$	normalized λ_j
$\tilde{\lambda}_j$	jth moment of live polymer radical with one undecomposed peroxide
$\underset{\sim}{\tilde{\lambda}}_j$	normalized $\tilde{\lambda}_j$
μ_j	jth moment of dead polymer
$\underset{\sim}{\mu}_j$	normalized μ_j
$\widetilde{\mu}_j$	jth moment of dead polymer with one undecomposed peroxide
$\underset{\sim}{\tilde{\mu}}_j$	normalized $\tilde{\mu}_j$

$\tilde{\tilde{\mu}}_j$	jth moment of dead polymer with two undecomposed peroxide	ρ_m	monomer density, g/L
$\tilde{\tilde{\mu}}_j$	normalized $\tilde{\tilde{\mu}}_j$	ρ_p	polymer density, g/L
$\tilde{\mu}^0$	parameter used to normalize radical and polymer moments	ρ_s	solvent density, g/L

The application of optimization function(s) is unique to optimal control, and provides extreme flexibility and enhanced capabilities to realize process objectives with greater performance. Together with the increase in computing power, and the development of more efficient optimal control techniques, research in the optimal control of industrial processes has begun to gain prominence.

It was established very early [1,2] that the performance of batch reactors, and their product properties depend strongly on reaction temperature. Many optimal control studies on batch reactors [3–6] have determined optimal temperatures, and provided deeper insights into reactor design, and optimal reactor performance. In case of batch polymerization, many researchers [7–10] have applied optimal control for the minimization of operation time, and the production of polymer with desired number and weight average molecular weights.

In the present study, we focus on the optimal control of the batch polymerization of MMA. The optimal control for the batch polymerization of MMA was first examined by King and Skaates [11]. They used trial and error simulations based on steady-state hypothesis for radical concentration, and an empirical gel effect model for bulk polymerization. Considering jacket temperature as a two-step control function of time, they determined optimal step-switching times under the constraints of 10% MMA conversion, and a specified maximum reactor temperature. Since then, several studies have been undertaken on the optimal control problem for MMA [12]. In general, these studies apply the calculus of variation on simplified and workable polymerization models to determine optimal control policies (i.e. functions of time) such as temperature, initiator and monomer concentrations. These policies optimize different variables, e.g. operation time, final monomer conversion, polymer molecular weight and polydispersity, subject to various constraints on process and polymer property.

An interesting study is by Ponnuswamy et al. [13], who determined as well as experimentally tested the optimal control policies for semi-batch MMA polymerization. They used the calculus of variation based on a simplified polymerization model to determine (i) optimal initiator concentration policy to minimize operation time, and (ii) optimal reaction temperature policies to minimize polydispersity. Final monomer concentration, and number average polymer molecular weight were specified as process constraints. Although experimental results generally agreed with optimal control predictions, discrepancies in number average polymer molecular weights were observed, thereby indicating the limitations of the simplified polymerization model employed.

There have been some optimal control studies on batch MMA polymerization using innovative approaches. Chang and Lai [8] proposed a two-step optimal control method, which first calculates number average degree of polymerization based on a final specification, and then uses a steady-state polymerization model to determine optimal control with non-linear programming. They applied this method for the optimal control of MMA polymerization in a batch reactor for specified final monomer conversion, number average degree of polymerization, and polydispersity. Tian et al. [14] used neural networks to determine optimal temperature policy for specified number average molecular weight, monomer conversion, and polydispersity for a batch MMA polymerization reactor. Chakravarthy et al. [15] optimally determined the reaction temperature as a control function of time for the bulk, batch polymerization of MMA with a monofunctional initiator. The composite objective was the weighted sum of operation time, and penalties on final monomer conversion and the number average polymer molecular weight with respect to their targeted values. In addition to Pontryagin's principle, the authors applied simple genetic algorithms [16] with restrictions on each discrete reaction temperature value (except the initial one) initially randomized around the preceding temperature value. Splines fitted on such values were used to obtain candidates for reaction temperature policies without extreme variations. Crossover operations were suitably restricted according to the number of discrete temperature values corresponding to the operation time. In another interesting study, Mankar et al. [17] applied realtime optimal control based on genetic algorithms to recover the bulk polymerization of MMA from a planned disturbance.

In this work, we determine the optimal control of free radical, solution polymerization of MMA with a bifunctional initiator. The temperature of heat exchange fluid

inside the jacket of reactor is used as a control function of time, or any specified independent variable depending on the objective. A detailed unsteady-state process model including the variation of temperature as well as reactor volume is used. Benzene is used as a solvent, and *N*,*N*′-bis[(4-*t*-butylazo-4-cyanovaleryl)oxyethyl]-azo-bis-formamide is used as a bifunctional initiator. This initiator is very useful in obtaining high initiation rates, and high polymer molecular weights [18]. A robust optimal control method based on genetic algorithms [19] is used to determine optimal control policies. This method iteratively uses genetic algorithms meshed with the size-variation of control function domain on logarithmic and linear scales, and has been successfully tested on challenging optimal control problems including polymerization [19,20].

Following are the main contributions presented in this work:

1. the determination of optimal control policies by suitably transforming the differential process model so that the independent variable is the one specified at the end of process. (This enables an additional parameter to be simultaneously optimized, and wider operation choices with four different objective functions realized in this work.)
2. the first time derivation and use of an unsteady-state process model based on previously used MMA polymerization kinetics with bifunctional initiation. (The reaction kinetics has been used in the past with pseudo-steady-state approximation only.)
3. the procedure to evaluate analytical Jacobians for the accurate solution of stiff differential process model.

Four different optimal control objectives are employed to enhance the performance of the batch MMA polymerization. Each objective optimizes a variable along with the specification or satisfaction of another. The objectives are: (i) maximization of monomer conversion in a specified operation time, (ii) minimization of operation time for specified, final monomer conversion, (iii) maximization of monomer conversion for a specified, final number average polymer molecular weight, and (iv) maximization of monomer conversion for a specified, final weight average polymer molecular weight. The temperature of heat-exchange fluid inside reactor jacket is used as a control function, which influences the temperature of reaction mixture.

2. Mathematical model

A detailed mathematical model is provided below for the batch polymerization of MMA in a non-isothermal batch reactor using a bifunctional initiator. Based on the reaction kinetics presented in Appendix A, the model comprises the equations of change of volume (V) and temperature (T) of reactants, the concentrations of monomer (m), initiator (i), solvent (s), inhibitor (z), and of the first three moments of regular radicals ($\lambda_0, \lambda_1, \lambda_2$), radicals with one undecomposed peroxide ($\tilde{\lambda}_0, \tilde{\lambda}_1, \tilde{\lambda}_2$), regular dead polymer molecules (μ_0, μ_1, μ_2), and dead polymer molecules with one and two undecomposed peroxides ($\tilde{\mu}_0, \tilde{\mu}_1, \tilde{\mu}_2$ and $\tilde{\tilde{\mu}}_0, \tilde{\tilde{\mu}}_1, \tilde{\tilde{\mu}}_2$). The equations are based on a free radical polymerization reaction mechanism given in Appendix A. The symbols in following expressions are defined in Nomenclature. The developed model that follows is very rigorous, and therefore is expected to yield better agreement between predictions and experimental results.

$$\frac{dV}{dt} = -K_p m(\lambda_0 + \tilde{\lambda}_0) V M_m \left[\frac{1}{\rho_p} - \frac{1}{\rho_m}\right] \tag{1}$$

$$\frac{dT}{dt} = \frac{-\Delta H K_p m(\lambda_0 + \tilde{\lambda}_0)}{\rho C_p} - \frac{UA(T - T_c)}{V \rho C_p} \tag{2}$$

$$\frac{dm}{dt} = -K_p m(\lambda_0 + \tilde{\lambda}_0) - \frac{m}{V}\frac{dV}{dt} \tag{3}$$

$$\frac{di}{dt} = 2K_{d1} i - \frac{i}{V}\frac{dV}{dt} \tag{4}$$

$$\frac{ds}{dt} = -K_{tf,s} s(\lambda_0 + \tilde{\lambda}_0) - \frac{s}{V}\frac{dV}{dt} \tag{5}$$

$$\frac{dz}{dt} = -K_{tf,z} z(\lambda_0 + \tilde{\lambda}_0) - \frac{z}{V}\frac{dV}{dt} \tag{6}$$

For moments of regular radicals:

$$\frac{d\lambda_0}{dt} = 2f_1 K_{d1} i + 2f_2 K_{d2}(\tilde{\mu}_0 + \tilde{\tilde{\mu}}_0) - K_t \lambda_0(\lambda_0 + \tilde{\lambda}_0) + (K_{tf,m} m + K_{tf,s} s)\tilde{\lambda}_0 - K_{tf,z} z \lambda_0 - \frac{\lambda_0}{V}\frac{dV}{dt} \tag{7}$$

$$\frac{d\lambda_1}{dt} = 2f_1 K_{d1} i + f_2 K_{d2}(\tilde{\mu}_0 + \tilde{\mu}_1 + 2\tilde{\tilde{\mu}}_0) + K_p m \lambda_0 - K_t \lambda_1(\lambda_0 + \tilde{\lambda}_0) + (K_{tf,m} m + K_{tf,s} s)(\lambda_0 - \lambda_1 + \tilde{\lambda}_0) - K_{tf,z} z \lambda_1 - \frac{\lambda_1}{V}\frac{dV}{dt} \tag{8}$$

$$\frac{d\lambda_2}{dt} = 2f_1 K_{d1} i + f_2 K_{d2}(\tilde{\mu}_0 + \tilde{\mu}_2 + 2\tilde{\tilde{\mu}}_0) + K_p m(\lambda_0 + 2\lambda_1) - K_t \lambda_2(\lambda_0 + \tilde{\lambda}_0) + (K_{tf,m} m + K_{tf,s} s)(\lambda_0 - \lambda_2 + \tilde{\lambda}_0) - K_{tf,z} z \lambda_2 - \frac{\lambda_2}{V}\frac{dV}{dt} \tag{9}$$

For moments of radicals with one undecomposed peroxide:

$$\frac{d\tilde{\lambda}_0}{dt} = 2f_1 K_{d1} i + 2f_2 K_{d2}\tilde{\tilde{\mu}}_0 - K_t \tilde{\lambda}_0(\lambda_0 + \tilde{\lambda}_0) - (K_{tf,m} m + K_{tf,s} s + K_{tf,z} z)\tilde{\lambda}_0 - \frac{\tilde{\lambda}_0}{V}\frac{dV}{dt} \tag{10}$$

$$\frac{d\tilde{\lambda}_1}{dt} = 2f_1K_{d1}i + 2f_2K_{d2}\tilde{\tilde{\mu}}_1 + K_p m\tilde{\lambda}_0 - K_t\tilde{\lambda}_1(\lambda_0 + \tilde{\lambda}_0) - (K_{tf,m}m + K_{tf,s}s + K_{tf,z}z)\tilde{\lambda}_1 - \frac{\tilde{\lambda}_1}{V}\frac{dV}{dt} \quad (11)$$

$$\frac{d\tilde{\lambda}_2}{dt} = 2f_1K_{d1}i + 2f_2K_{d2}\tilde{\tilde{\mu}}_2 + K_p m(\tilde{\lambda}_0 + 2\tilde{\lambda}_1) - K_t\tilde{\lambda}_2(\lambda_0 + \tilde{\lambda}_0) - (K_{tf,m}m\tilde{\lambda}_2 + K_{tf,s}s + K_{tf,z}z)\tilde{\lambda}_2 - \frac{\tilde{\lambda}_2}{V}\frac{dV}{dt} \quad (12)$$

For moments of dead polymer molecules:

$$\frac{d\mu_0}{dt} = \frac{K_{t,c}\lambda_0^2}{2} + K_{t,d}\lambda_0(\lambda_0 + \tilde{\lambda}_0) + (K_{tf,m}m + K_{tf,s}s + K_{tf,z}z)\lambda_0 - \frac{\mu_0}{V}\frac{dV}{dt} \quad (13)$$

$$\frac{d\mu_1}{dt} = K_{t,c}\lambda_0\lambda_1 + K_{t,d}\lambda_1(\lambda_0 + \tilde{\lambda}_0) + (K_{tf,m}m + K_{tf,s}s + K_{tf,z}z)\lambda_1 - \frac{\mu_1}{V}\frac{dV}{dt} \quad (14)$$

$$\frac{d\mu_2}{dt} = K_{t,c}(\lambda_0\lambda_2 + \lambda_1^2) + K_{t,d}\lambda_2(\lambda_0 + \tilde{\lambda}_0) + (K_{tf,m}m + K_{tf,s}s + K_{tf,z}z)\lambda_2 - \frac{\mu_2}{V}\frac{dV}{dt} \quad (15)$$

For moments of dead polymer molecules with one undecomposed peroxide molecule:

$$\frac{d\tilde{\mu}_0}{dt} = -K_{d2}\tilde{\mu}_0 + K_{t,c}\lambda_0\tilde{\lambda}_0 + K_{t,d}\tilde{\lambda}_0(\lambda_0 + \tilde{\lambda}_0) + (K_{tf,m}m + K_{tf,s}s + K_{tf,z}z)\tilde{\lambda}_0 - \frac{\tilde{\mu}_0}{V}\frac{dV}{dt} \quad (16)$$

$$\frac{d\tilde{\mu}_1}{dt} = -K_{d2}\tilde{\mu}_1 + K_{t,c}(\lambda_0\tilde{\lambda}_1 + \lambda_1\tilde{\lambda}_0) + K_{t,d}\tilde{\lambda}_1(\lambda_0 + \tilde{\lambda}_0) + (K_{tf,m}m + K_{tf,s}s + K_{tf,z}z)\tilde{\lambda}_1 - \frac{\tilde{\mu}_1}{V}\frac{dV}{dt} \quad (17)$$

$$\frac{d\tilde{\mu}_2}{dt} = -K_{d2}\tilde{\mu}_2 + K_{t,c}(\lambda_2\tilde{\lambda}_0 + 2\lambda_1\tilde{\lambda}_1 + \lambda_0\tilde{\lambda}_2) + K_{t,d}\tilde{\lambda}_2(\lambda_0 + \tilde{\lambda}_0) + (K_{tf,m}m + K_{tf,s}s + K_{tf,z}z)\tilde{\lambda}_2 - \frac{\tilde{\mu}_2}{V}\frac{dV}{dt} \quad (18)$$

For moments of dead polymer molecules with two undecomposed peroxide molecules:

$$\frac{d\tilde{\tilde{\mu}}_0}{dt} = -2K_{d2}\tilde{\tilde{\mu}}_0 + \frac{K_{t,c}\tilde{\lambda}_0^2}{2} - \frac{\tilde{\tilde{\mu}}_0}{V}\frac{dV}{dt} \quad (19)$$

$$\frac{d\tilde{\tilde{\mu}}_1}{dt} = -2K_{d2}\tilde{\tilde{\mu}}_1 + K_{t,c}\tilde{\lambda}_0\tilde{\lambda}_1 - \frac{\tilde{\tilde{\mu}}_1}{V}\frac{dV}{dt} \quad (20)$$

$$\frac{d\tilde{\tilde{\mu}}_2}{dt} = -2K_{d2}\tilde{\tilde{\mu}}_2 + K_{t,c}(\tilde{\lambda}_0\tilde{\lambda}_2 + \tilde{\lambda}_1^2) - \frac{\tilde{\tilde{\mu}}_2}{V}\frac{dV}{dt} \quad (21)$$

Let us define normalized state variables as

$$\underset{\sim}{V} = 1 - \frac{V}{V^0}, \quad \underset{\sim}{T} = 1 - \frac{T + 273.15}{T^0 + 273.15},$$
$$\underset{\sim}{m} = 1 - \frac{m}{m^0}, \quad \underset{\sim}{i} = 1 - \frac{i}{i^0}, \quad \underset{\sim}{s} = 1 - \frac{s}{s^0},$$
$$\underset{\sim}{z} = 1 - \frac{z}{z^0}, \quad \underset{\sim}{\lambda}_j = 1 - \frac{\lambda_j}{\mu^0}, \quad \underset{\sim}{\tilde{\lambda}}_j = 1 - \frac{\tilde{\lambda}_j}{\mu^0},$$
$$\underset{\sim}{\mu}_j = 1 - \frac{\mu_j}{\mu^0}, \quad \underset{\sim}{\tilde{\mu}}_j = 1 - \frac{\tilde{\mu}_j}{\mu^0}, \quad \underset{\sim}{\tilde{\tilde{\mu}}}_j = 1 - \frac{\tilde{\tilde{\mu}}_j}{\mu^0}; \quad j = 0, 1, 2 \quad (22)$$

where V^0, T^0, m^0, i^0, s^0 and z^0 are the initial values of V, T, m, i, s and z, respectively, and μ^0 is a parameter used to normalize radical and polymer moments. Then the equations of change for the normalized state variables are given by

$$\frac{d\underset{\sim}{y}_j}{dt} = \left\{ \begin{array}{ll} -\frac{1}{y_j^0}\frac{dy_j}{dt}, & \text{if } y_j^0 \neq 0 \\ 0, & \text{if } y_j^0 = 0 \end{array} \right\}; \quad j = 0, 1, 2, \ldots, 20 \quad (23)$$

where $\underset{\sim}{y}_j$ is the normalized form of a state variable, y_j, with the normalization factor, y_j^0.

3. Optimal control objectives

Based on the above mathematical model, four different optimal control objectives for batch MMA polymerization are presented in this section. The temperature of heat-exchange fluid in reactor jacket (or "jacket temperature") is considered as a control function of a specified parameter. An inequality constraint in the form of an upper limit to the temperature of reactants is enforced as

$$T \leqslant T_{max} \quad (24)$$

There are two additional inequality constraints in the form of lower and upper limits to jacket temperature, i.e.,

$$T_{j,min} \leqslant T_j \leqslant T_{j,max} \quad (25)$$

3.1. Objective 1

The optimal control objective is to determine the control policy for jacket temperature that would maximize monomer conversion in a specified batch operation time (t_f), i.e., the performance index,

$$\underset{max}{J} = X(t_f) = X_f \quad (26)$$

In Eq. (26), X is monomer conversion given by

$$X = 1 - \frac{mV}{m^0V^0} = 1 - (1 - \underset{\sim}{m})(1 - \underset{\sim}{V}) \quad (27)$$

This objective requires the satisfaction of Eqs. (1)–(7), (10), (13), (16) and (19); or their normalized form given by Eq. (23).

3.2. Objective 2

The optimal control objective is to determine the control policy for jacket temperature that would minimize operation time for a specified, final monomer conversion expressed in terms of fractional reduction in monomer concentration ($\underset{\sim}{m}_{\mathrm{f}}$), i.e., the performance index,

$$\underset{\min}{J} = t(\underset{\sim}{m}_{\mathrm{f}}) = t_{\mathrm{f}} \tag{28}$$

This objective requires the transformation of Eqs. (1)–(21) so that the independent variable is the fractional reduction in monomer concentration ($\underset{\sim}{m}$). The transformed equations are given by

$$\frac{\mathrm{d}t}{\mathrm{d}\underset{\sim}{m}} = \left[\frac{\mathrm{d}\underset{\sim}{m}}{\mathrm{d}t}\right]^{-1} \quad \text{for} \quad j = 2 \tag{29}$$

$$\frac{\mathrm{d}\underset{\sim}{y}_j}{\mathrm{d}\underset{\sim}{m}} = \left[\frac{\mathrm{d}\underset{\sim}{m}}{\mathrm{d}t}\right]^{-1} \frac{\mathrm{d}\underset{\sim}{y}_j}{\mathrm{d}t}; \quad j = 0, 1, 3, 4, \ldots, 20 \tag{30}$$

with time as a new state variable.

3.3. Objective 3

The optimal control objective is to determine the control policy for jacket temperature that would maximize monomer conversion for a specified, final weight average polymer molecular weight ($\overline{M}_{\mathrm{n,f}}$), i.e., the performance index,

$$\underset{\max}{J} = X(\overline{M}_{\mathrm{n,f}}) = X_{\mathrm{f}} \tag{31}$$

This objective requires the satisfaction of Eqs. (1)–(21) after their transformation so that the independent variable is number average polymer molecular weight ($\overline{M}_{\mathrm{n}}$). The transformed equations are given by

$$\frac{\mathrm{d}\underset{\sim}{y}_j}{\mathrm{d}\overline{M}_{\mathrm{n}}} = \left[\frac{\mathrm{d}\overline{M}_{\mathrm{n}}}{\mathrm{d}t}\right]^{-1} \frac{\mathrm{d}\underset{\sim}{y}_j}{\mathrm{d}t}; \quad j = 0, 1, \ldots, 20 \tag{32}$$

where

$$\overline{M}_{\mathrm{n}} = \overline{M}_{\mathrm{m}} \left(\frac{\mu_1 + \tilde{\mu}_1 + \tilde{\tilde{\mu}}_1 + \lambda_1 + \tilde{\lambda}_1}{\mu_0 + \tilde{\mu}_0 + \tilde{\tilde{\mu}}_0 + \lambda_0 + \tilde{\lambda}_0} \right) \tag{33}$$

$$\begin{aligned} \frac{\mathrm{d}\overline{M}_{\mathrm{n}}}{\mathrm{d}t} = {} & \frac{M_{\mathrm{m}}\mu^0}{\mu_0 + \tilde{\mu}_0 + \tilde{\tilde{\mu}}_0 + \lambda_0 + \tilde{\lambda}_0} \\ & \times \left[\overline{M}_{\mathrm{n}} \left(\frac{\mathrm{d}\underset{\sim}{\mu}_0}{\mathrm{d}t} + \frac{\mathrm{d}\underset{\sim}{\tilde{\mu}}_0}{\mathrm{d}t} + \frac{\mathrm{d}\underset{\sim}{\tilde{\tilde{\mu}}}_0}{\mathrm{d}t} + \frac{\mathrm{d}\underset{\sim}{\lambda}_0}{\mathrm{d}t} + \frac{\mathrm{d}\underset{\sim}{\tilde{\lambda}}_0}{\mathrm{d}t} \right) \right. \\ & \left. - \left(\frac{\mathrm{d}\underset{\sim}{\mu}_1}{\mathrm{d}t} + \frac{\mathrm{d}\underset{\sim}{\tilde{\mu}}_1}{\mathrm{d}t} + \frac{\mathrm{d}\underset{\sim}{\tilde{\tilde{\mu}}}_1}{\mathrm{d}t} + \frac{\mathrm{d}\underset{\sim}{\tilde{\lambda}}_1 \mathrm{d}t \underset{\sim}{\tilde{\lambda}}_1}{\mathrm{d}t} \right) \right] \end{aligned} \tag{34}$$

The additional equation of change for time as a state variable is given by

$$\frac{\mathrm{d}t}{\mathrm{d}\overline{M}_{\mathrm{n}}} = \left[\frac{\mathrm{d}\overline{M}_{\mathrm{n}}}{\mathrm{d}t}\right]^{-1} \quad \text{for } j = 21 \tag{35}$$

3.4. Objective 4

The optimal control objective is to determine the control policy for jacket temperature that would maximize monomer conversion for a specified, final weight average polymer molecular weight ($\overline{M}_{\mathrm{w,f}}$), i.e., the performance index,

$$\underset{\max}{J} = X(\overline{M}_{\mathrm{w,f}}) = X_{\mathrm{f}} \tag{36}$$

This objective requires the satisfaction of Eqs. (1)–(21) after their transformation so that the independent variable is weight average polymer molecular weight ($\overline{M}_{\mathrm{w}}$). The transformed equations are given by

$$\frac{\mathrm{d}\underset{\sim}{y}_j}{\mathrm{d}\overline{M}_{\mathrm{w}}} = \left[\frac{\mathrm{d}\overline{M}_{\mathrm{w}}}{\mathrm{d}t}\right]^{-1} \frac{\mathrm{d}\underset{\sim}{y}_j}{\mathrm{d}t}; \quad j = 0, 1, \ldots, 20 \tag{37}$$

where

$$\overline{M}_{\mathrm{w}} = M_{\mathrm{m}} \left(\frac{\mu_2 + \tilde{\mu}_2 + \tilde{\tilde{\mu}}_2 + \lambda_2 + \tilde{\lambda}_2}{\mu_1 + \tilde{\mu}_1 + \tilde{\tilde{\mu}}_1 + \lambda_1 + \tilde{\lambda}_1} \right) \tag{38}$$

$$\begin{aligned} \frac{\mathrm{d}\overline{M}_{\mathrm{w}}}{\mathrm{d}t} = {} & \frac{M_{\mathrm{m}}\mu^0}{\mu_1 + \tilde{\mu}_1 + \tilde{\tilde{\mu}}_1 + \lambda_1 + \tilde{\lambda}_1} \\ & \times \left[\overline{M}_{\mathrm{w}} \left(\frac{\mathrm{d}\underset{\sim}{\mu}_1}{\mathrm{d}t} + \frac{\mathrm{d}\underset{\sim}{\tilde{\mu}}_1}{\mathrm{d}t} + \frac{\mathrm{d}\underset{\sim}{\tilde{\tilde{\mu}}}_1}{\mathrm{d}t} + \frac{\mathrm{d}\underset{\sim}{\lambda}_1}{\mathrm{d}t} + \frac{\mathrm{d}\underset{\sim}{\tilde{\lambda}}_1}{\mathrm{d}t} \right) \right. \\ & \left. - \left(\frac{\mathrm{d}\underset{\sim}{\mu}_2}{\mathrm{d}t} + \frac{\mathrm{d}\underset{\sim}{\tilde{\mu}}_2}{\mathrm{d}t} + \frac{\mathrm{d}\underset{\sim}{\tilde{\tilde{\mu}}}_2}{\mathrm{d}t} + \frac{\mathrm{d}\underset{\sim}{\lambda}_2}{\mathrm{d}t} \frac{\mathrm{d}\underset{\sim}{\tilde{\lambda}}_2}{\mathrm{d}t} \right) \right] \end{aligned} \tag{39}$$

The additional equation of change for time as a state variable is given by

$$\frac{\mathrm{d}t}{\mathrm{d}\overline{M}_{\mathrm{w}}} = \left[\frac{\mathrm{d}\overline{M}_{\mathrm{w}}}{\mathrm{d}t}\right]^{-1} \quad \text{for} \quad j = 21 \tag{40}$$

For Objectives 2–4, the above transformations of the process model, Eqs. (1)–(21), enable its integration in the range of a specified independent variable (which is not time) up to its specified, final value.

4. Integration of batch process model

The four optimal control objectives described above require the integration of corresponding equations of change with different independent variables ($t, \underset{\sim}{m}, \overline{M}_{\mathrm{n}}$ and $\overline{M}_{\mathrm{w}}$) for performance index evaluations. These equations are very stiff and non-linear. In this work, they were numerically integrated using semi-implicit Bader–

Deuflhard algorithm, and adaptive step-size control [21]. Analytical Jacobians were employed for integration. The equations to evaluate the elements of Jacobian corresponding to each optimal control objective are provided in the next section.

4.1. Equations to evaluate Jacobians

Equations for the analytical evaluation of Jacobian are for normalized state variables, and time (for Objectives 2–4) with respect to the independent variable depending on an optimal control objective. Using the start-up values, y_j^0, and the basic Jacobian elements, $\frac{d}{dy_k}\left(\frac{dy_j}{dt}\right)$, the Jacobian elements are sequentially calculable as described below.

4.1.1. Jacobian for Objective 1

For all state variables, the elements of the Jacobian are given by

$$\frac{d}{d\underset{\sim}{y}_k}\left(\frac{d\underset{\sim}{y}_j}{dt}\right) = \left\{\begin{array}{ll} \dfrac{y_k^0}{y_j^0}\dfrac{d}{dy_k}\left(\dfrac{dy_j}{dt}\right), & \text{if } y_j^0 > 0 \\ 0, & \text{if } y_j^0 = 0 \end{array}\right\}; \quad j,k = 0,1,2,\ldots,20 \tag{41}$$

Eq. (41) is same for other optimal control objectives until the independent variable of Eqs. (1)–(21), which initially is time, is changed to $\underset{\sim}{m}$, $\overline{M}_n$ and $\overline{M}_w$ for Objectives 2, 3 and 4, respectively. Time then becomes a new state variable. For this transformation, the new independent variable must be non-zero. The Jacobians for Objectives 2–4 are then sequentially calculable as follows:

4.1.2. Jacobian for Objective 2

The Jacobian elements for time, corresponding to $j = 0$, are given by

$$\frac{d}{dt}\left(\frac{dt}{d\underset{\sim}{m}}\right) = 0 \quad \text{for } k = 2 \tag{42}$$

$$\frac{d}{d\underset{\sim}{y}_k}\left(\frac{dt}{d\underset{\sim}{m}}\right) = -m^0 y_k^0\left[\frac{dm}{dt}\right]^{-2}\frac{d}{dy_k}\left(\frac{dm}{dt}\right); \quad k = 0,1,3,4\ldots,20 \tag{43}$$

The Jacobian elements for remaining state variables, corresponding to $j = 0,1,3,4,\ldots,20$, are given by

$$\frac{d}{d\underset{\sim}{y}_k}\left(\frac{d\underset{\sim}{y}_j}{d\underset{\sim}{m}}\right) = -\frac{1}{y_j^0}\frac{dy_j}{dt}\frac{d}{d\underset{\sim}{y}_k}\left(\frac{dt}{d\underset{\sim}{m}}\right) + \alpha; \quad k = 0,1,\ldots,20 \tag{44}$$

In Eq. (44),

$$\alpha = \left\{\begin{array}{ll} -m^0\left[\dfrac{dm}{dt}\right]^{-1}\dfrac{y_k^0}{y_j^0}\dfrac{d}{dy_k}\left(\dfrac{dy_j}{dt}\right), & \text{if } y_j^0 > 0 \\ 0, & \text{if } y_j^0 = 0 \end{array}\right. \tag{45}$$

4.1.3. Jacobian for Objective 3

Let $\overline{M}_n$ correspond to $j = 21$ before the transformation of the independent variable. Then the basic Jacobian elements for $\overline{M}_n$ are given by

$$\frac{d}{d\overline{M}_n}\left(\frac{d\overline{M}_n}{dt}\right) = 0 \quad \text{for } k = 21 \tag{46}$$

$$\begin{aligned}\frac{d}{dy_k}\left(\frac{d\overline{M}_n}{dt}\right) = {} & \frac{M_m}{\mu_0+\tilde{\mu}_0+\tilde{\tilde{\mu}}_0+\lambda_0+\tilde{\lambda}_0}\left[\frac{d}{dy_k}\left(\frac{d\mu_1}{dt}\right)\right. \\ & + \frac{d}{dy_k}\left(\frac{d\tilde{\mu}_1}{dt}\right) + \frac{d}{dy_k}\left(\frac{d\tilde{\tilde{\mu}}_1}{dt}\right) + \frac{d}{dy_k}\left(\frac{d\lambda_1}{dt}\right) \\ & \left. + \frac{d}{dy_k}\left(\frac{d\tilde{\lambda}_1}{dt}\right)\right] - \frac{M_m\overline{M}_n}{\mu_0+\tilde{\mu}_0+\tilde{\tilde{\mu}}_0+\lambda_0+\tilde{\lambda}_0} \\ & \times\left[\frac{d}{dy_k}\left(\frac{d\mu_0}{dt}\right) + \frac{d}{dy_k}\left(\frac{d\tilde{\mu}_0}{dt}\right) + \frac{d}{dy_k}\left(\frac{d\tilde{\tilde{\mu}}_0}{dt}\right)\right. \\ & \left. + \frac{d}{dy_k}\left(\frac{d\lambda_0}{dt}\right) + \frac{d}{dy_k}\left(\frac{d\tilde{\lambda}_0}{dt}\right)\right] + \beta_0; \\ & k = 0,1,\ldots,20\end{aligned} \tag{47}$$

In Eq. (47),

$$\beta_0 = \left\{\begin{array}{l} \dfrac{-M_m}{(\mu_0+\tilde{\mu}_0+\tilde{\tilde{\mu}}_0+\lambda_0+\tilde{\lambda}_0)^2}\left[\left(\dfrac{d\mu_1}{dt}+\dfrac{d\tilde{\mu}_1}{dt}+\dfrac{d\tilde{\tilde{\mu}}_1}{dt}+\dfrac{d\lambda_1}{dt}+\dfrac{d\tilde{\lambda}_1}{dt}\right)\right. \\ \quad \left.-2\overline{M}_n\left(\dfrac{d\mu_0}{dt}+\dfrac{d\tilde{\mu}_0}{dt}+\dfrac{d\tilde{\tilde{\mu}}_0}{dt}+\dfrac{d\lambda_0}{dt}+\dfrac{d\tilde{\lambda}_0}{dt}\right)\right] \\ \quad \text{for } y_k = \mu_0,\ \tilde{\mu}_0,\ \tilde{\tilde{\mu}}_0,\ \lambda_0,\tilde{\lambda}_0 \\ \dfrac{-M_m}{(\mu_0+\tilde{\mu}_0+\tilde{\tilde{\mu}}_0+\lambda_0+\tilde{\lambda}_0)^2}\left(\dfrac{d\mu_0}{dt}+\dfrac{d\tilde{\mu}_0}{dt}+\dfrac{d\tilde{\tilde{\mu}}_0}{dt}+\dfrac{d\lambda_0}{dt}+\dfrac{d\tilde{\lambda}_0}{dt}\right) \\ \quad \text{for } y_k = \mu_1,\tilde{\mu}_1,\tilde{\tilde{\mu}}_1,\lambda_1,\tilde{\lambda}_1 \\ 0, \quad \text{for remaining } y_k\text{s} \end{array}\right. \tag{48}$$

After the transformation of the independent variable to $\overline{M}_n$, time becomes a new state variable (refer Eq. (35)). The Jacobian elements for time, corresponding to $j = 21$, are given by

$$\frac{d}{d\underset{\sim}{y}_k}\left(\frac{dt}{d\overline{M}_n}\right) = y_k^0\left[\frac{d\overline{M}_n}{dt}\right]^{-2}\frac{d}{dy_k}\left(\frac{d\overline{M}_n}{dt}\right); \quad k = 0,1,\ldots,20 \tag{49}$$

$$\frac{d}{dt}\left(\frac{dt}{d\overline{M}_n}\right) = 0 \quad \text{for } k = 21 \tag{50}$$

The Jacobian elements for remaining state variables, corresponding to $j = 0,1,\ldots,20$, are given by

$$\frac{\mathrm{d}}{\mathrm{d}\underset{\sim}{y}_k}\left(\frac{\mathrm{d}\underset{\sim}{y}_j}{\mathrm{d}\overline{M}_\mathrm{n}}\right) = -\frac{1}{y_j^0}\frac{\mathrm{d}y_j}{\mathrm{d}t}\frac{\mathrm{d}}{\mathrm{d}\underset{\sim}{y}_k}\left(\frac{\mathrm{d}t}{\mathrm{d}\overline{M}_\mathrm{n}}\right) + \gamma_0; \quad k = 0, 1, 2, \ldots, 20 \tag{51}$$

$$\frac{\mathrm{d}}{\mathrm{d}t}\left(\frac{\mathrm{d}\underset{\sim}{y}_j}{\mathrm{d}\overline{M}_\mathrm{n}}\right) = 0 \quad \text{for } k = 21 \tag{52}$$

In Eq. (51),

$$\gamma_0 = \begin{cases} \left[\dfrac{\mathrm{d}\overline{M}_\mathrm{n}}{\mathrm{d}t}\right]^{-1}\dfrac{y_k^0}{y_j^0}\dfrac{\mathrm{d}}{\mathrm{d}y_k}\left(\dfrac{\mathrm{d}y_j}{\mathrm{d}t}\right), & \text{if } y_j^0 > 0 \\ 0, & \text{if } y_j^0 = 0 \end{cases} \tag{53}$$

4.1.4. Jacobian for Objective 4

Let $\overline{M}_\mathrm{w}$ correspond to $j = 21$ before the transformation of the independent variable. Then the basic Jacobian elements for $\overline{M}_\mathrm{w}$ are given by

$$\frac{\mathrm{d}}{\mathrm{d}\overline{M}_\mathrm{w}}\left(\frac{\mathrm{d}\overline{M}_\mathrm{w}}{\mathrm{d}t}\right) = 0 \quad \text{for } k = 21 \tag{54}$$

$$\frac{\mathrm{d}}{\mathrm{d}y_k}\left(\frac{\mathrm{d}\overline{M}_\mathrm{w}}{\mathrm{d}t}\right) = \frac{\overline{M}_\mathrm{m}}{\mu_1 + \tilde{\mu}_1 + \tilde{\tilde{\mu}}_1 + \lambda_1 + \tilde{\lambda}_1}\left[\frac{\mathrm{d}}{\mathrm{d}y_k}\left(\frac{\mathrm{d}\mu_2}{\mathrm{d}t}\right) + \frac{\mathrm{d}}{\mathrm{d}y_k}\left(\frac{\mathrm{d}\tilde{\mu}_2}{\mathrm{d}t}\right) + \frac{\mathrm{d}}{\mathrm{d}y_k}\left(\frac{\mathrm{d}\tilde{\tilde{\mu}}_2}{\mathrm{d}t}\right) + \frac{\mathrm{d}}{\mathrm{d}y_k}\left(\frac{\mathrm{d}\lambda_2}{\mathrm{d}t}\right) + \frac{\mathrm{d}}{\mathrm{d}y_k}\left(\frac{\mathrm{d}\tilde{\lambda}_2}{\mathrm{d}t}\right)\right] - \frac{M_\mathrm{m}\overline{M}_\mathrm{w}}{\mu_1 + \tilde{\mu}_1 + \tilde{\tilde{\mu}}_1 + \lambda_1 + \tilde{\lambda}_1} \times \left[\frac{\mathrm{d}}{\mathrm{d}y_k}\left(\frac{\mathrm{d}\mu_1}{\mathrm{d}t}\right) + \frac{\mathrm{d}}{\mathrm{d}y_k}\left(\frac{\mathrm{d}\tilde{\mu}_1}{\mathrm{d}t}\right) + \frac{\mathrm{d}}{\mathrm{d}y_k}\left(\frac{\mathrm{d}\tilde{\tilde{\mu}}_1}{\mathrm{d}t}\right) + \frac{\mathrm{d}}{\mathrm{d}y_k}\left(\frac{\mathrm{d}\lambda_1}{\mathrm{d}t}\right) + \frac{\mathrm{d}}{\mathrm{d}y_k}\left(\frac{\mathrm{d}\tilde{\lambda}_1}{\mathrm{d}t}\right)\right] + \beta_1; \quad k = 0, 1, 2, \ldots, 20 \tag{55}$$

In Eq. (55),

$$\beta_1 = \begin{cases} \dfrac{-M_\mathrm{m}}{(\mu_1 + \tilde{\mu}_1 + \tilde{\tilde{\mu}}_1 + \lambda_1 + \tilde{\lambda}_1)^2}\left[\left(\dfrac{\mathrm{d}\mu_2}{\mathrm{d}t} + \dfrac{\mathrm{d}\tilde{\mu}_2}{\mathrm{d}t} + \dfrac{\mathrm{d}\tilde{\tilde{\mu}}_2}{\mathrm{d}t} + \dfrac{\mathrm{d}\lambda_2}{\mathrm{d}t} + \dfrac{\mathrm{d}\tilde{\lambda}_2}{\mathrm{d}t}\right) - 2\overline{M}_\mathrm{w}\left(\dfrac{\mathrm{d}\mu_1}{\mathrm{d}t} + \dfrac{\mathrm{d}\tilde{\mu}_1}{\mathrm{d}t} + \dfrac{\mathrm{d}\tilde{\tilde{\mu}}_1}{\mathrm{d}t} + \dfrac{\mathrm{d}\lambda_1}{\mathrm{d}t} + \dfrac{\mathrm{d}\tilde{\lambda}_1}{\mathrm{d}t}\right)\right] & \text{for } y_k = \mu_1, \tilde{\mu}_1, \tilde{\tilde{\mu}}_1, \lambda_1, \tilde{\lambda}_1 \\ \dfrac{-M_\mathrm{m}}{(\mu_1 + \tilde{\mu}_1 + \tilde{\tilde{\mu}}_1 + \lambda_1 + \tilde{\lambda}_1)^2}\left(\dfrac{\mathrm{d}\mu_1}{\mathrm{d}t} + \dfrac{\mathrm{d}\tilde{\mu}_1}{\mathrm{d}t} + \dfrac{\mathrm{d}\tilde{\tilde{\mu}}_1}{\mathrm{d}t} + \dfrac{\mathrm{d}\lambda_1}{\mathrm{d}t} + \dfrac{\mathrm{d}\tilde{\lambda}_1}{\mathrm{d}t}\right) & \text{for } y_k = \mu_2, \tilde{\mu}_2, \tilde{\tilde{\mu}}_2, \lambda_2, \tilde{\lambda}_2 \\ 0, & \text{for remaining } y_k\text{s} \end{cases} \tag{56}$$

After the transformation of the independent variable to $\overline{M}_\mathrm{w}$, time becomes a new state variable (refer Eq. (40)). The Jacobian elements for time, corresponding to $j = 21$, are given by

Table 1
Model parameters used in calculations

Parameter	Value or expression	Source
f	0.6	This study
i^0, mol/L	4.13×10^{-2}	
m^0, mol/L	1.7648	
s^0, mol/L	8.4692	
T^0, °C	70 (Objectives 1 and 2), 0 (Objectives 3 and 4)	
T_max, °C	80	
$T_\mathrm{j,max}$, °C	120	
$T_\mathrm{j,min}$, °C	4 (Objectives 1 and 2), −20 (Objectives 3 and 4)	
V^0, L	1	
z^0, mol/L	10^{-5}	
μ^0	10^{-6}	
$K_\mathrm{tf,s}$, L/mol min	$1.58 \times 10^{-5} K_\mathrm{p}$	
$K_\mathrm{tf,z}$, L/mol min	$10^6 K_\mathrm{p}$	
M_m, g/mol	100.12 (for MMA)	
M_s, g/mol	78.11 (for benzene)	
K_d1, K_d2, min^{-1}	$3 \times 10^{11}\exp[-1.1299 \times 10^4/(T + 273.15)]$	Simionescu et al. [18]
UA, J/min K	6.5475×10^2	Villalobos et al. [22]
$-\Delta H$, J/mol	5.546×10^4	Brandrup et al. [23]
$K_\mathrm{tf,m}$, L/mol min	$5.358 \times 10^{-2}\exp[-1.1273 \times 10^3/(T + 273.15)]$	Kalfas et al. [24]
ρ_m, g/L	$309.85 \times 0.25357^{-[1-(T + 273.15)/564]^{0.28571}}$	Yaws [25]
ρ_s, g/L	$300.9 \times 0.2677^{-[1-(T + 273.15)/562.16]^{0.2818}}$	
C_p, J/g K	$4.2416 \times 10^3 + 1.08 \times 10^2(T + 273.15) - 3.1588 \times 10^{-1}(T + 273.15)^2 + 3.7804 \times 10^{-4}(T + 273.15)^3$	
ρ_p, g/L	$1.18 \times 10^3 - (T + 273.15)$	Ahn et al. [26]

$$\frac{\mathrm{d}}{\mathrm{d}\underset{\sim}{y}_k}\left(\frac{\mathrm{d}t}{\mathrm{d}\overline{M}_\mathrm{w}}\right) = y_k^0\left[\frac{\mathrm{d}\overline{M}_\mathrm{w}}{\mathrm{d}t}\right]^{-2}\frac{\mathrm{d}}{\mathrm{d}y_k}\left(\frac{\mathrm{d}\overline{M}_\mathrm{w}}{\mathrm{d}t}\right);\quad k=0,1,\ldots,20 \tag{57}$$

$$\frac{\mathrm{d}}{\mathrm{d}t}\left(\frac{\mathrm{d}t}{\mathrm{d}\overline{M}_\mathrm{w}}\right) = 0 \quad \text{for } k=21 \tag{58}$$

The Jacobian elements for remaining state variables, corresponding to $j=0,1,\ldots,20$, are given by

$$\frac{\mathrm{d}}{\mathrm{d}\underset{\sim}{y}_k}\left(\frac{\mathrm{d}\underset{\sim}{y}_j}{\mathrm{d}\overline{M}_\mathrm{w}}\right) = -\frac{1}{y_j^0}\frac{\mathrm{d}y_j}{\mathrm{d}t}\frac{\mathrm{d}}{\mathrm{d}\underset{\sim}{y}_k}\left(\frac{\mathrm{d}t}{\mathrm{d}\overline{M}_\mathrm{w}}\right)+\gamma_1;\quad k=0,1,\ldots,20 \tag{59}$$

$$\frac{\mathrm{d}}{\mathrm{d}t}\left(\frac{\mathrm{d}\underset{\sim}{y}_j}{\mathrm{d}\overline{M}_\mathrm{w}}\right) = 0 \quad \text{for } k=21 \tag{60}$$

In Eq. (59),

$$\gamma_1 = \begin{cases}\left[\dfrac{\mathrm{d}\overline{M}_\mathrm{w}}{\mathrm{d}t}\right]^{-1}\dfrac{y_k^0}{y_j^0}\dfrac{\mathrm{d}}{\mathrm{d}y_k}\left(\dfrac{\mathrm{d}y_j}{\mathrm{d}t}\right), & \text{if } y_j^0>0\\ 0, & \text{if } y_j^0=0\end{cases} \tag{61}$$

For the integration of equations of change, μ^0 was adjusted so that the difference between the value of independent variable (e.g. $\overline{M}_\mathrm{n}$ or $\overline{M}_\mathrm{w}$), and that calculated using other state variables (e.g. from Eq. (33) or (38)) is negligible. For Objectives 2–4, the transformation of process model was done as soon as the new independent variable achieved a finite value lying within the first stage of optimal control.

Various parameters used in calculations are provided in Table 1. The gel effect models for propagation and termination rate coefficients are provided in Appendices B and C, respectively. The reactants for polymerization are the MMA (monomer), *N*,*N*′-bis[(4-*t*-butylazo-4-cyanovaleryl)oxyethyl]-azo-bis-formamide (bifunctional initiator), benzene (solvent), and trace amount of some impurity (inhibitor). The product is the polymer, poly(MMA). No experimental data are available for the free radical polymerization of MMA using bifunctional initiator. As such, we will compare the results of optimal control with the base case simulation of batch MMA polymerization with bifunctional initiator at a constant reaction temperature of 70 °C. This isothermal temperature of base case is one of the normally considered temperatures for MMA polymerization.

5. Optimal control method

The mathematical model presented above for the batch polymerization of MMA is highly non-linear. Furthermore, due to the inequality constraints of Eqs. (24) and (25), the relation between the performance index and jacket temperature for Objectives 1–4 would not necessarily be unimodal and continuous for the four optimal control objectives.

To realize these difficult objectives, a robust optimal control method based on genetic algorithms [19] was applied. This optimal control method iteratively uses the three genetic operations of selection, crossover and mutation in the size-varying domain of control function with logarithmic and linear mappings. The method does not require any input of feasible control solution, or any auxiliary condition. This method has been successfully applied earlier for the optimal control of ethylene polymerization in an industrial tubular reactor [20]. Further details of this method may be found in Upreti [19].

In this work, the temperature of heat-exchange fluid inside reactor jacket (or jacket temperature) was employed as a control function of specified independent variable. Based on numerical experiments, the number of control stages or step values was optimally selected with respect to the quality of optimal result as well as computation time for a single run of optimal control algorithm. The optimal results obtained with less than five steps were inferior than those with five steps. On the other hand, the results with more than five steps increased the computation time (with a 3.06 GHz personal computer having 1 GB random access memory) to more than a week, but with marginal improvements. Hence, jacket temperature was considered to be a series of five discrete step values equispaced in the range of independent variable. The number of step values, the mathematical model of bulk, batch polymerization reactor with its parameters, and the process constraints of Eqs. (24) and (25) were input to the optimal control method. These inputs are needed to evaluate the performance index for a given control function. The application of the method yielded an optimal control function through the stochastic application of genetic operators on a randomly generated set of control functions constrained by Eq. (25). Since the method generates optimal control functions within the control domain, the constraints of Eq. (25) are satisfied automatically. The method eliminates any control function for which any other process constraint (Eq. (24) in this application) is violated during the evaluation of corresponding performance index.

6. Results

The optimal control results for the four objectives are summarized and compared with the base case in Table 2. Note that the specified values of average polymer molecular weights in Objectives 3 and 4 are simply not attainable in base case.

Table 2
Summary of optimal control results

Objective	Specification	J in base case	Optimal J	% Improvement in J
1	$t_f = 100$ min	$X_f = 65.9\%$	$X_{f,\max} = 85.6\%$	30
2	$X_f = 70\%$	$t_f = 111.9$ min	$t_{f,\min} = 63.9$ min	43
3	$\overline{M}_{n,f} = 6.7 \times 10^4$	Not attainable	$X_{f,\max} = 67.9\%$	–
4	$\overline{M}_{w,f} = 1.5 \times 10^5$	Not attainable	$X_{f,\max} = 49.7\%$	–

6.1. Results for Objective 1

The optimal jacket temperature policy was determined, which maximizes final monomer (MMA) conversion during the specified batch polymerization time of 100 min. Fig. 1 shows the optimal policy, which maximizes final monomer conversion to 85.6%. This value is about 30% higher than the monomer conversion in base case. The figure also shows how the temperature policy gets improved with the iterations of the optimal control method. It is observed that the optimal policy reaches close to the maximum allowable reactor temperature of 80 °C.

Fig. 2 shows the change in optimal reactor temperature, and monomer conversion with time, which correspond to the optimal jacket temperature policy. Corresponding variables for base case are also shown in the figure. It is observed that optimal reactor temper-

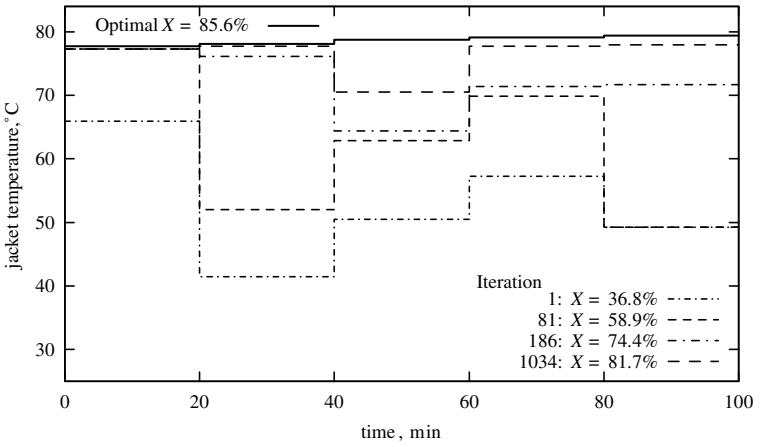

Fig. 1. Optimal reactor jacket temperature versus time for Objective 1.

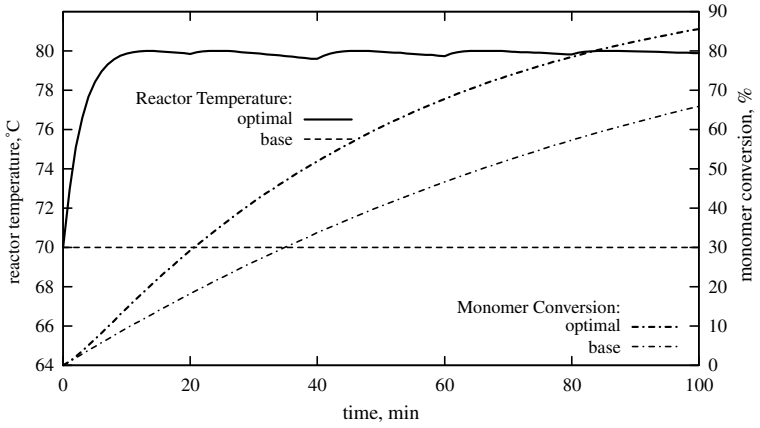

Fig. 2. Reactor temperature and monomer conversion versus time for Objective 1.

ature increases very quickly, and gets close to its upper limit of 80 °C in less than 10 min. In the following time, the temperature is observed to be in phase with the optimal jacket temperature (Fig. 1) in the lower vicinity of its upper limit. This fact indicates that high reaction temperatures are needed in all control stages in order to increase overall polymerization, and achieve high monomer conversion. This behavior shows the strong influence of jacket temperature on reaction temperature, and explains why optimal jacket temperature does not surpass the upper limit of reactor temperature. The proximity of optimal reactor temperature to optimal jacket temperature is governed by the overall heat transfer coefficient used in this work, and is specific to the reactor configuration modeled and simulated earlier [27]. For the reactor with a lower value of heat transfer coefficient and consequently greater heat accumulation in an exothermic polymerization, the optimal jacket temperatures would be lower such that the optimal reactor temperature does not exceed its upper limit anytime. In the present case, optimal reactor temperature is always well within the prescribed upper limit, which is specified through Eq. (24). For time greater than zero, the optimal value of reactor temperature exceeds that for base case. Correspondingly, optimal monomer conversion, for time greater than zero, is always higher than the monomer conversion for base case.

The optimal number and weight average polymer molecular weights ($\overline{M}_n$ and $\overline{M}_w$) versus time are respectively shown in Figs. 3 and 4 along with those for base case. It is observed that optimal $\overline{M}_n$ as well as $\overline{M}_w$ values are always lower than respectively those in base case. In comparison to base case, the final values of optimal $\overline{M}_n$ and $\overline{M}_w$ are reduced by about 42% and 36%, respectively. This reduction indicates that optimal reactor temperature, which is higher than the reactor temperature in

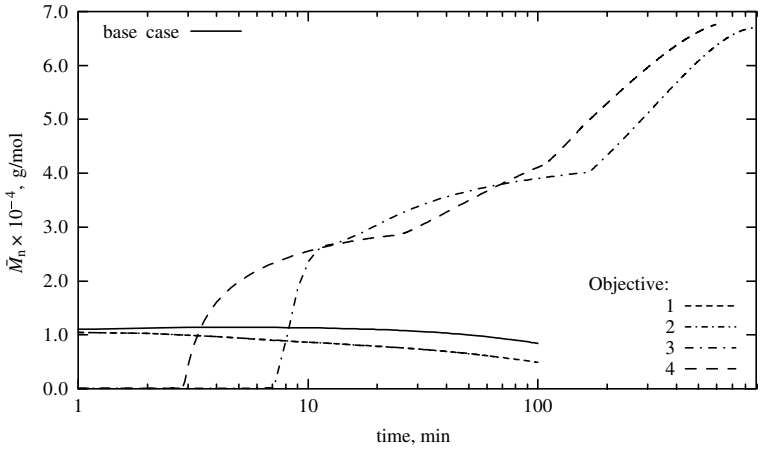

Fig. 3. Optimal number average molecular weight versus time for Objectives 1–4.

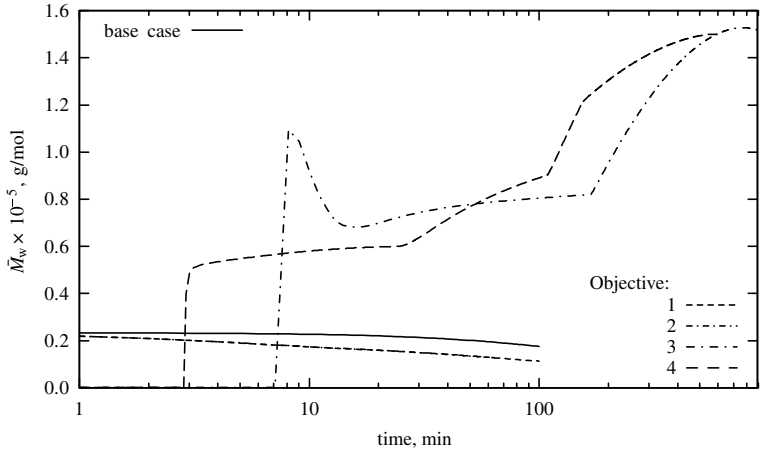

Fig. 4. Optimal weight average molecular weight versus time for Objectives 1–4.

base case, has favored the generation of polymer molecules with smaller chain lengths.

6.2. Results for Objective 2

The optimal jacket temperature policy was determined, which minimizes batch polymerization time for the specified, final monomer conversion of 70%. Shown in Fig. 5, the optimal policy is again close to the maximum allowable reactor temperature of 80 °C; similar to what was observed for Objective 1. Moreover, the time-averaged value of optimal jacket temperature is approximately same as that in case of Objective 1. This similarity of optimal jacket temperature is reasonable because the realization of each of Objectives 1 and 2 requires the maximization of overall rate of monomer conversion.

Optimal reactor temperature, shown in Fig. 6, closely follows optimal jacket temperature after the first control stage. This behavior was observed earlier in case of Objective 1. Corresponding to optimal jacket temperature, the optimal value of the operation time is 63.9 min, which is a reduction by 43% relative to base case.

Fig. 7 shows optimal monomer conversion. For Objectives 1 and 2, the conversion overlaps, and is always higher than that for base case. The optimal number and weight average polymer molecular weights ($\overline{M}_n$ and $\overline{M}_w$) are respectively shown in Figs. 3 and 4. The changes in monomer conversion, and average molecular weights with time almost coincide with respectively those in case of Objective 1. The reason is that corresponding optimal reactor and jacket temperatures for Objective 1 and 2 are not much different, and are close to their upper limit.

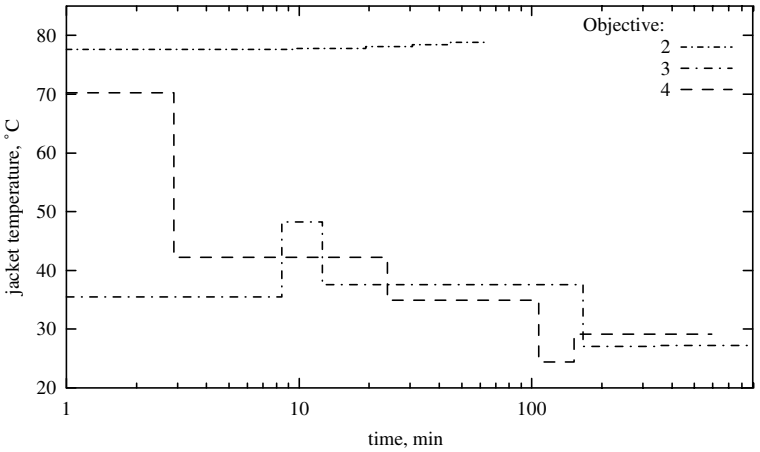

Fig. 5. Optimal jacket temperature versus time for Objectives 2–4.

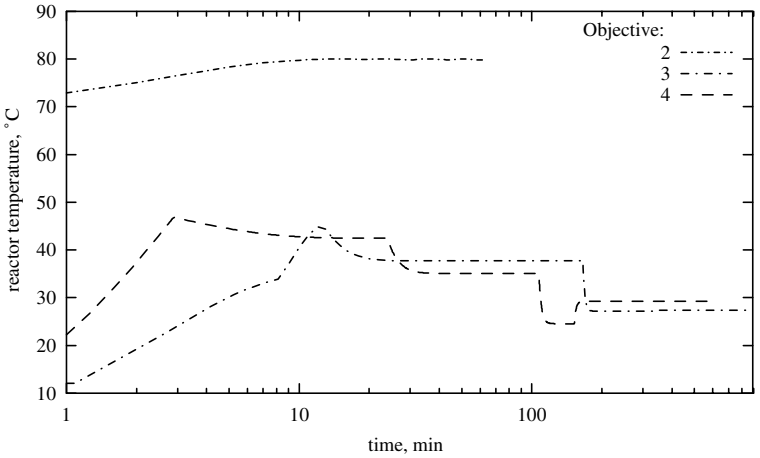

Fig. 6. Optimal reactor temperature versus time for Objectives 2–4.

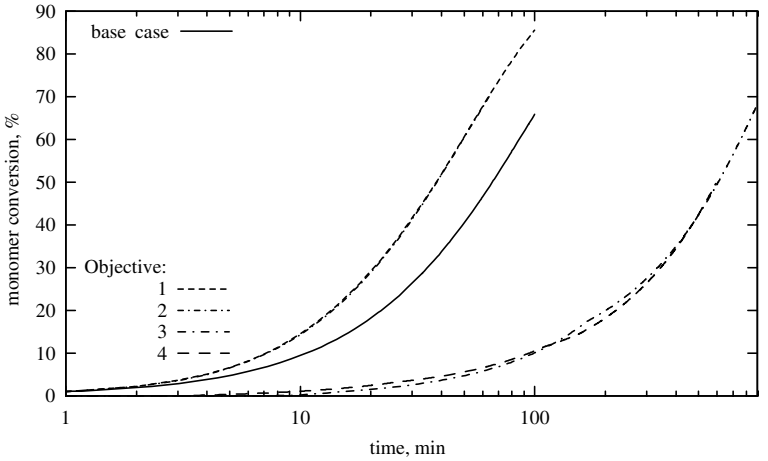

Fig. 7. Optimal monomer conversion versus time for Objectives 1–4 (graphs for Objectives 1 and 2 overlap).

6.3. Results for Objective 3

The optimal jacket temperature policy was determined, which maximizes the final monomer conversion with the specified final number average molecular weight ($\overline{M}_{n,f}$) of 6.7×10^4 g/mol. It may be noted that, as seen in Fig. 3, this high value of $\overline{M}_n$ is not achievable in base case. In general, the time needed to obtain polymer of a specified $\overline{M}_{n,f}$ increases with a decrease in reaction temperature. To provide extended application time for optimal control through jacket temperature, and to facilitate higher monomer conversion during that time, the initial temperature of reactor was set at a low value of 0 °C. Furthermore, wider range (for lower values) was made available to jacket temperature by reducing its lower limit to −20 °C.

Fig. 5 shows the resulting optimal control policy for jacket temperature, which spans 884.6 min of operation time, and yields the final monomer conversion of 67.9%. Although the lower limit for jacket temperature is −20 °C, its lowest optimal value is above 25 °C. At the beginning optimal jacket temperature is 35.5 °C, and rises to 48.3 °C, which is the highest for all control stages. The temperature declines later on. It is noticed that the third control stage is of longer duration than other stages. The reason is that control stages are equispaced over the specified independent variable, $\overline{M}_n$, which undergoes the slowest change with time in the third control stage (see Fig. 3). In fact, the rates of change of both $\overline{M}_n$ (Fig. 3) and $\overline{M}_w$ (Fig. 4) with time are reduced in the third control stage. The rate of change of $\overline{M}_w$ is initially negative in the third control stage. This behavior is due to the higher optimal jacket and reactor temperatures in the third stage, which favor the generation of polymer molecules with smaller chain lengths. The trend of optimal jacket temperature after the first control stage is closely followed by corresponding optimal reactor temperature as seen in Fig. 6.

The change in optimal monomer conversion with time, as seen in Fig. 7, is very small up to the first half of the third stage after which the conversion rises to the final value of 67.9%.

6.4. Results for Objective 4

The optimal jacket temperature policy was determined, which maximizes the final monomer conversion with the specified final weight average molecular weight ($\overline{M}_{w,f}$) of 1.5×10^5 g/mol. It may be noted again that, as seen in Fig. 4, this high value of $\overline{M}_w$ is not achievable in base case. Optimal control results for this objective were obtained for the same initial reactor temperature, and the lower limit of jacket temperature that were used for Objective 3. The realization of the present optimal control objective with high monomer conversions is lower than the previous Objective 3. The reason is the initial increase of $\overline{M}_w$ with time being higher than that of $\overline{M}_n$. This limitation results in polymerization that meets the specification of $\overline{M}_{w,f}$ very quickly, thereby reducing the time available for optimal control through jacket temperature.

Fig. 5 shows the resulting optimal jacket temperature versus time which spans 592.4 min of operation time, and yields a final monomer conversion of 49.7%. This value (as well as operation time) is lower than that for Objective 3, thereby indicating the effect of the above mentioned limitation. The variation in optimal jacket temperature with time is different from that in Objective 3. The temperature is the highest in the first control stage after which it declines except in the last stage. This trend is closely followed by optimal reactor temperature as seen in Fig. 6. Optimal $\overline{M}_n$ (Fig. 3), $\overline{M}_w$ (Fig. 4) for this objective are observed to increase monotonically with time. The change in optimal monomer conversion with time, as seen in Fig. 7, is similar to that in case of Objective 3.

7. Conclusion

The optimal control of MMA polymerization with a bifunctional initiator was determined in a non-isothermal batch reaction with volume variation. The following four optimal control objectives were realized: (i) maximization of monomer conversion in a specified operation time, (ii) minimization of operation time for specified, final monomer conversion, (iii) maximization of monomer conversion for a specified, final number average polymer molecular weight, and (iv) maximization of monomer conversion for a specified, final weight average polymer molecular weight. The temperature of heat-exchange fluid in jacket of reactor was utilized as a control function of a specified independent variable. The process constraints were maximum reactor temperature, and the upper and lower limits to the temperature of heat-exchange fluid.

The above objectives were formulated to help provide wider choices for polymer production simultaneously with the optimum efficiency of operation. Equations were provided to suitably transform the model of batch MMA polymerization with a bifunctional initiator in the range of specified variable other than time, and to evaluate the elements of Jacobian. Based on the model, the four optimal control objectives were realized using a robust method based on genetic algorithms. The results of optimal control showed significant performance improvements compared to base case without optimal control.

Acknowledgment

The financial support of the Natural Sciences and Engineering Research Council of Canada is gratefully acknowledged.

Appendix A. MMA polymerization kinetics

Based on the approach of Villalobos et al. [28], Gao and Penlidis [29], and Dhib et al. [27], following is the kinetics used in this work:

Chemical initiation:

$$I \xrightarrow{2K_{d1}} R_{in}^{\cdot} + \widetilde{R}_{in}^{\cdot} \tag{62}$$

$$R_{in}^{\cdot} + M \xrightarrow{K_1} R_1^{\cdot} \tag{63}$$

$$\widetilde{R}_{in}^{\cdot} + M \xrightarrow{K_2} \widetilde{R}_1^{\cdot} \tag{64}$$

$$\widetilde{P}_l \xrightarrow{K_{d2}} R_{in}^{\cdot} + R_l^{\cdot}, \quad l \geqslant 1 \tag{65}$$

$$\widetilde{\widetilde{P}}_l \xrightarrow{2K_{d2}} R_{in}^{\cdot} + \widetilde{R}_l^{\cdot}, \quad l \geqslant 1 \tag{66}$$

Propagation:

$$R_l^{\cdot} + M \xrightarrow{K_p} R_{l+1}^{\cdot}, \quad l \geqslant 1 \tag{67}$$

$$\widetilde{R}_l^{\cdot} + M \xrightarrow{K_p} \widetilde{R}_{l+1}^{\cdot}, \quad l \geqslant 1 \tag{68}$$

Termination by combination:

$$R_l^{\cdot} + R_k^{\cdot} \xrightarrow{K_{t,c}} P_{l+k}, \quad l,k \geqslant 1 \tag{69}$$

$$R_l^{\cdot} + \widetilde{R}_k^{\cdot} \xrightarrow{K_{t,c}} \widetilde{P}_{l+k}, \quad l,k \geqslant 1 \tag{70}$$

$$\widetilde{R}_l^{\cdot} + \widetilde{R}_k^{\cdot} \xrightarrow{K_{t,c}} \widetilde{\widetilde{P}}_{l+k}, \quad l,k \geqslant 1 \tag{71}$$

Termination by disproportionation:

$$R_l^{\cdot} + R_k^{\cdot} \xrightarrow{K_{t,d}} P_l + P_k, \quad l,k \geqslant 1 \tag{72}$$

$$R_l^{\cdot} + \widetilde{R}_k^{\cdot} \xrightarrow{K_{t,d}} P_l + \widetilde{P}_k, \quad l,k \geqslant 1 \tag{73}$$

$$\widetilde{R}_l^{\cdot} + \widetilde{R}_k^{\cdot} \xrightarrow{K_{t,d}} \widetilde{P}_l + \widetilde{P}_k, \quad l,k \geqslant 1 \tag{74}$$

Transfer to monomer:

$$R_l^{\cdot} + M \xrightarrow{K_{tf,m}} P_l + R_1^{\cdot}, \quad l \geqslant 1 \tag{75}$$

$$\widetilde{R}_l^{\cdot} + M \xrightarrow{K_{tf,m}} \widetilde{P}_l + R_1^{\cdot}, \quad l \geqslant 1 \tag{76}$$

Transfer to solvent:

$$R_l^{\cdot} + S \xrightarrow{K_{tf,s}} P_l + R_1^{\cdot}, \quad l \geqslant 1 \tag{77}$$

$$\widetilde{R}_l^{\cdot} + S \xrightarrow{K_{tf,s}} \widetilde{P}_l + R_1^{\cdot}, \quad l \geqslant 1 \tag{78}$$

Transfer to inhibitor (or impurity):

$$R_l^{\cdot} + Z \xrightarrow{K_{tf,z}} P_l + Z^{\cdot}, \quad l \geqslant 1 \tag{79}$$

$$R_l^{\cdot} + Z \xrightarrow{K_{tf,z}} \widetilde{P}_l + Z^{\cdot}, \quad l \geqslant 1 \tag{80}$$

Appendix B. Rate coefficient for propagation

Rate coefficient for propagation is given by

$$K_p = K_{p,1} \times K_{p,2} \quad [\text{L/mol min}] \tag{81}$$

where, from Louie et al. [12]:

$$K_{p,1} = 2.95 \times 10^7 \times \exp\left(\frac{-2.1892 \times 10^3}{T + 273.15}\right) \quad [\text{L/mol min}] \tag{82}$$

from Schmidt and Ray [30]:

$$K_{p,2} = \begin{cases} 7.1 \times 10^{-5} \exp(171.53 V_f), & \text{if } V_f < V_{fpc} \\ 1, & \text{if } V_f \geqslant V_{fpc} \end{cases} \tag{83}$$

$$V_{fpc} = 0.05 \tag{84}$$

and from Ahn et al. [26]:

$$V_f = 0.025 + V_{f,m} + V_{f,p} + V_{f,s} \quad (85)$$

$$V_{f,m} = \frac{(T - T_{g,m}) m M_m \times 10^{-3}}{\rho_m} \quad (86)$$

$$V_{f,p} = \frac{(T - T_{g,p})(m^0 - m) M_m \times 4.8 \times 10^{-4}}{\rho_p} \quad (87)$$

$$V_{f,s} = \frac{(T - T_{g,s}) s M_s \times 10^{-3}}{\rho_s} \quad (88)$$

Appendix C. Rate coefficient for termination

Rate coefficient for termination is given by

$$K_t = K_{t,c} + K_{t,d} = K_{t,1} \times K_{t,2} \quad [\text{L/mol min}] \quad (89)$$

where, from Kalfas et al. [24]:

$$\frac{K_{t,d}}{K_{t,c}} = 1.49 \times 10^5 \exp\left(\frac{-2.0498 \times 10^3}{T + 273.15}\right) \quad (90)$$

from Ahn et al. [26]:

$$K_{t,1} = 3.12 \times 10^{10} \times \exp\left(\frac{-7.0156 \times 10^2}{T + 273.15}\right) \quad [\text{L/mol min}] \quad (91)$$

and from Schmidt and Ray [30]:

$$K_{t,2} = \begin{cases} 2.3 \times 10^{-6} \exp(75 V_f), & \text{if } V_f < V_{ftc} \\ 0.10575 \exp(17.15 V_f - 0.01715 T), & \text{if } V_f \geqslant V_{ftc} \end{cases} \quad (92)$$

$$V_{ftc} = 0.1856 - 2.965 \times 10^{-4} T \quad (93)$$

References

[1] Denbigh KG. Optimum temperature sequences in reactors. Chem Eng Sci 1958;8:125–32.

[2] Aris R. On Denbigh's optimum temperature sequence. Chem Eng Sci 1960;12:56–64.

[3] Luus R, Okongwu ON. Towards practical optimal control of batch reactors. Chem Eng J 1999;75:1–9.

[4] Logsdon JS, Biegler LT. A relaxed reduced space for sqp strategy for dynamic optimization problems. Comp Chem Eng 1993;17:367–72.

[5] Luus R. Optimal control of batch reactors by iterative dynamic programming. J Proc Control 1994;4(4):218–26.

[6] Bojkov B, Luus R. Optimal control of nonlinear systems with unspecified final times. Chem Eng Sci 1996;51:905–19.

[7] Hicks JM, Mohan A, Ray WH. The optimal control of polymerization reactors. Can J Chem Eng 1969;47:590–8.

[8] Chang JS, Lai JL. Computation of optimal temperature policy for molecular weight control in a batch polymerization reactor. Ind Eng Chem Res 1992;31(3):861.

[9] Thomas IM, Kiparissides C. Computation of the near-optimal temperature and initiator policies for a batch polymerization reactor. Can J Chem Eng 1984;62(2):284–91.

[10] O'Driscoll KF, Ponnuswamy SR. Optimization of batch polymerization reactor as the final stage of conversion. ii molecular weight constraint. J Appl Polym Sci 1990;39(6):1299–308.

[11] King PE, Skaates JM. Two-position control of a batch prepolymerization. Ind Eng Chem Proc Des Dev 1969;8(1):114–9.

[12] Louie BM, Carratt GM, Soong DS. Modeling the free radical solution and bulk polymerization of methyl methacrylate. J Appl Polym Sci 1985;30:3985–4012.

[13] Ponnuswamy SR, Shah SL, Kipaissides CA. Computer optimal control of batch polymerization reactors. Ind Eng Chem Res 1987;26(11):2229–36.

[14] Tian Y, Zhang J, Morris J. Modeling and optimal control of a batch polymerization reactor using a hybrid stacked recurrent neural network model. Ind Eng Chem Res 2001;40:4525–35.

[15] Chakravarthy SSS, Saraf DN, Gupta SK. Use of genetic algorithms in the optimization of free radical polymerizations exhibiting the Trommsdorff effect. J Appl Polym Sci 1997;63:529–48.

[16] Deb K. Optimization for engineering design: algorithms and examples. New Delhi, India: Prentice Hall of India; 1995.

[17] Mankar RB, Saraf DN, Gupta SK. On-line optimizing control of bulk polymerization of methyl methacrylate: some experimental results for heater failure. J Appl Polym Sci 2002;85:2350–60.

[18] Simionescu IC, Popa AA, Comanita E, Pastravanu M. Kinetics of methyl methacrylate polymerization initiated with *n,n′*-bis[(4-*t*-butylazo-4-cyanovaleryl)oxyethyl]-azo-bis-formamide. Brit Polym J 1990;23:347–51.

[19] Upreti SR. A new robust technique for optimal control of chemical engineering processes. Comp Chem Eng 2004;28(8):1325–36.

[20] Yao FZ, Lohi A, Upreti SR, Dhib R. Modeling, simulation and optimal control of ethylene polymerization in non-isothermal, highpressure tubular reactors. Int J Chem Reactor Eng 2004;2(A16).

[21] Press WH, Teukolsky SA, Vetterling WT, Flannery BP. Numerical recipes in C++. The art of scientific computing. 2nd ed. New York: Cambridge University Press; 2002. p. 719–27.

[22] Villalobos MA, Hamielec AE, Wood PE. Bulk and suspension polymerization of styrene in the presence of *n*-pentane. An evaluation of monofunctional and bifunctional initiation. J Appl Polym Sci 1993;50(2):327–43.

[23] Brandrup J, Immergut EH, Grulke EA, editors. Polymer handbook. 4th ed. New York: Wiley-Interscience; 1999.

[24] Kalfas G, Yuan H, Ray WH. Modeling and experimental studies of aqueous suspension polymerization processes. 2. Experiments in batch reactor. Ind Eng Chem Res 1993;32:1831–8.

[25] Yaws CL. Chemical properties handbook. New York: McGraw-Hill; 1999.

[26] Ahn SM, Chang SC, Rhee H. Application of optimal temperature trajectory to batch pmma polymerization reactor. J Appl Polym Sci 1998;69:59–68.

[27] Dhib R, Gao J, Penlidis A. Simulation of free radical bulk/solution homopolymerization using mono- and bi-functional initiators. Polym Reactor Eng 2000;8(4):299–464.
[28] Villalobos MA, Hamielec AE, Wood PE. Kinetic model for short-cycle bulk styrene polymerization through bifunctional initiators. J Appl Polym Sci 1991;42(3):629–41.
[29] Gao J, Penlidis A. A comprehensive simulator/database package for reviewing free radical homopolymerizations. J Macromol Sci Rev Macromol Chem Phys 1996;C36:199–404.
[30] Schmidt AD, Ray WH. The dynamic behavior of continuous polymerization reactors-I. Chem Eng Sci 1981;36:1401–10.